

## Automated sawtooth detection with multi-signal analysis

A. Gude, M. Maraschek, P. Eulenberg, V. Igoshine, ASDEX Upgrade Team

Max Planck Institute for Plasma Physics, Boltzmannstr. 2, D-85748 Garching, Germany

**Introduction** Sawtooth crashes (SCs) are periodic relaxations of the core plasma which occur when the central safety factor,  $q_0$ , is below 1. They consist of a ramp-phase during which temperatures and particle densities evolve slowly, and a fast crash that basically flattens these quantities inside the mixing radius,  $\rho_{mix}$ . For peaked pre-crash profiles, the SC decreases the values close to the magnetic axis and increases them just inside  $\rho_{mix}$ . At the inversion radius,  $\rho_{inv}$ , the values remain unchanged. SCs decrease the core confinement, but they also help to avoid impurity accumulation in the hot plasma centre, and to get rid of helium ash in a future fusion reactor. Large sawtooth crashes can trigger neoclassical tearing modes (NTMs), which gets more likely for long sawtooth periods. Sawtooth control therefore does not necessarily aim at avoiding sawteeth but at keeping them small and frequent.

**Motivation** Sawtooth control requires reliable SC detection. Suitable diagnostics are ECE for electron temperature,  $T_e$ , and Soft X-ray (SXR) detectors for radiation. The advantages of ECE are its local measurement and the dependence on just one plasma quantity, but the plasma coverage is often incomplete and ECE signals are prone to failure when  $n_e$  is close to/above the cut-off density. The line-integration of SXR signals affects the observed  $\rho_{inv}$ . Combined with the dependence on various quantities, especially the non-linear dependence on  $T_e$ , SXR signals are more difficult to interpret than those of ECE. In the presence of tungsten (W) impurities and central heating, SXR profiles are often hollow (local minimum in the centre) because of hollow tungsten density,  $n_W$ , profiles. A SC then leads to increase

of  $n_W$  on axis and decrease further out in such cases [1]. With peaked  $T_e$  profiles, there are competing crash effects: central SXR emissivity is increased with  $n_W$  but decreased with  $T_e$ , leading to a large variety of SC characteristics. In ITER, with a W divertor and central  $\alpha$  particle heat-

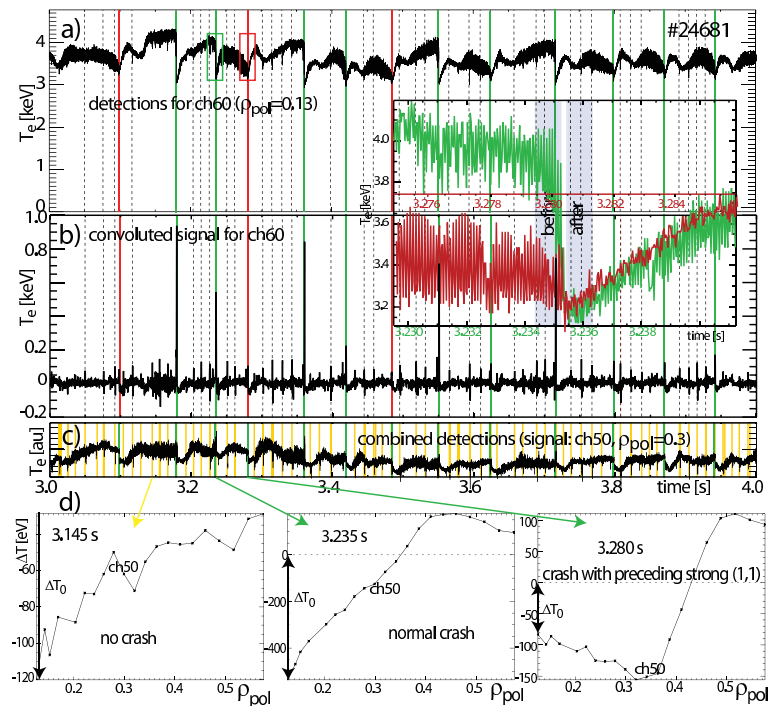


Figure 1: a) Time trace and edge detections for most central ECE channel. Detected SCs are marked in green, missed ones in red. b) convolution of (a), c) combined detections using all channels shown in (d), d) crash profiles for an ELM, a normal and a mode-preceded crash. Small inset: zoom of boxes in a).

ing, such conditions can be expected.

Moreover, in ASDEX Upgrade in plasmas with central wave heating, it has been observed, that strong ( $m=1, n=1$ ) MHD instabilities can affect  $T_e$  before the SC [2], leading to strongly reduced drops (figure 1 a)). In order to detect such SCs, the detection threshold has to be low, which will lead to detection of more events that are not SCs (false positives: FPs). Figure 2 b) shows that losses in the most central ECE channel for FPs are of the same order as for mode-preceded crashes, for which the highest losses occur at larger  $\rho_{pol}$  (figure 1 d). These circumstances require a suitable discrimination between SCs and other detected events. We focus on SXR signals because of their availability in most plasma conditions and the excellent plasma coverage. The goal is reliable SC detection for statistical analysis or real-time application.

**SC detection** The necessary quantity that a sawtooth detection must deliver with sufficient precision is the crash time point,  $t_{SC}$ . Once this is known, other SC characteristics can be extracted, e.g., inversion positions or amplitude. Imprecise  $t_{SC}$  can lead to wrong extracted values. The acceptable deviation ( $\approx 0.3$  ms), is slightly larger than the crash duration (mostly  $\leq 0.1$  ms) to account for precursor effects. The first task is to detect fast changes (edges) in detector signals observing the SC. These edges can be jumps both to smaller or to larger values, depending on the measurement position (inside or outside  $\rho_{inv}$ ) and on the SC type (normal or inverted crash). Edge detection is a task often used in image processing [3]. Our task is simpler in the sense that we only consider edges in one dimension (time).

Since the crash appears (almost) simultaneously in all channels, we can use the second dimension (space) to improve the detection reliability. Figure 1 a) shows that detection in the central channel alone misses some SCs, which are found when a larger range of signals is used (fig 1 c). Furthermore, there are other events that cause abrupt changes in the signals, which must be discriminated. Therefore, pure edge detection, sophisticated as it may be, is not sufficient for reliable detection of the whole range of SCs. We have to use crash characteristics for the decision if an event is likely to be a SC or not. Our SC detection is performed in three steps: 1) Edge detection in individual signals, 2) Correlation of detected events in a range of signals, 3) Analysis of crash profile (difference of radial distributions after minus before the crash) for a wide signal range to discriminate FPs.

**Edge detection** The edge detection consists of two parts. First the signal is convoluted with a suitable kernel function. Following [3], we chose the first derivative of a Gaussian with width  $\sigma_k$ , (cut off at  $\pm 3.5\sigma_k$ ). This transfers edges in the signal to peaks in the convoluted signal, (see figure 1 a),b)). The peak heights are equal to the edge heights in the original signal for a normalized kernel. Then the decision has to be made, which of the local extrema in the convoluted signals are due to edges and which are due to remaining noise. A threshold for the peak height has to be defined. This must be self-adapting to the discharge conditions for automated detection. One can use the noise level of the original signal or of the convoluted

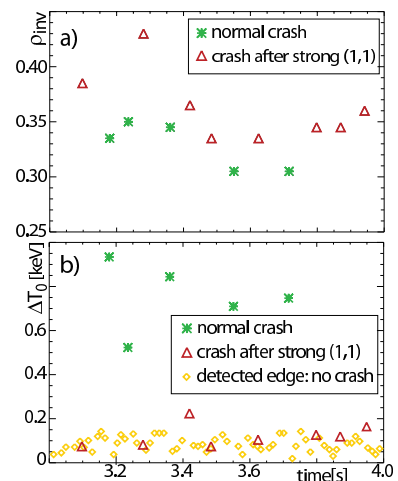


Figure 2: a)  $\rho_{inv}$  of crashes of figure 1, b)  $T_0$  for all detected edges of figure 1 c).

one for this purpose. The estimation of the noise level from the signal level itself is error-prone, because MHD modes and other events, including the crash precursor, a (1,1) mode, itself, which have to be regarded as noise for SC detection, are not caught.

We present a self-adaptive threshold for peak discrimination using the kurtosis, a measure for the peakedness of a statistical distribution  $X = x_1, \dots, x_i, \dots, x_n$ , defined as:  $\kappa(x) = 1/n \sum ((x_i - \mu)/\sigma_x)^4$ , where  $\mu$  is the mean value of  $X$  and  $\sigma_x$  the square root of the variance of  $X$ . It is calculated for slices of the convoluted signal, called kurtosis windows. For kurtosis windows with only Gaussian noise,  $\kappa = 3$ . For  $X$  with many data close to  $\mu$  and also far away from  $\mu$  (e.g., a signal with a large peak and some noise in the remaining kurtosis window),  $\kappa \gg 3$ . Since  $\kappa$  is invariant to changed order of data points, the position of the peak has to be determined beforehand. We do this by searching for the absolute extremum in each kurtosis window and shift the window in time such that the extremum is in its middle.

**Edge detection parameters** The kurtosis window has to be larger than the peak width, which is determined by the kernel width. Otherwise there is no noise contribution and  $\kappa < 3$ . Analysis of the ratio of kurtosis over edge height in an otherwise constant (but noisy) signal reveals that reliable edge detection is possible only for kurtosis windows that are at least 8 to 10 times longer than the kernel. The kernel width must be large enough for effective noise filtering. On the other hand, it must be small in order to detect the crash but not the recovery phase. The latter can be much shorter than the sawtooth period, but in ASDEX Upgrade it is not shorter than 2 ms. We chose a full kernel width of 1.5 ms, corresponding to  $\sigma_k \approx 0.214$  ms. For NBI heated discharges with plasma rotation frequencies around 10 kHz this is long enough to smooth precursor oscillations. This choice requires a kurtosis window of at least 12 ms ( $\pm 6$  ms around the peak centre), allowing to detect SCs with minimum distance  $\approx 6.5$  ms. The kurtosis threshold,  $\kappa_{min}$ , has to reject most noise peaks. Because of statistical scatter and other perturbations, it must be significantly larger than 3. We chose  $\kappa_{min} = 4.5$ , which is rather low and results in a few more false detections in this first step, but we will discriminate those in the last step.

**Correlation of detected events** The central time points of all kurtosis windows for which the threshold is exceeded, are analysed for all detection channels together. Events that are less than 0.3 ms apart are combined to one event. Events detected in only one signal are ignored. The average over all contributing time points, weighted with the peak height, gives the combined  $t_{SC}$ . For a larger maximum time distance, detections around the crash can lead to imprecise  $t_{SC}$ .

**Event discrimination** Last, we have to decide whether a detected edge results from a SC. Typical assumptions are that a SC reduces  $T_e$  and radiation in the centre and that  $\rho_{inv}$  is close to the  $q = 1$  surface and therefore does not change rapidly. Both criteria are no longer applicable in the presence of tungsten impurities and central heating: A SC can also lead to positive edges in central channels, and figure 2 a) shows that  $\rho_{inv}$  can vary strongly from crash to crash. For SXR, the variation of  $\rho_{inv}$  is even stronger and more common.

In any case, a SC causes redistribution. Therefore, we analyse the crash profile, which is represented by the convoluted signal values ( $c$ ) at  $t_{SC}$  ( $p := c(t_{SC})$ ). We chose a profile range inside  $\rho_m := \rho_{pol,max} = 0.7$ , in order to include the full mixing region. The crash profiles, originally only defined at the measurement positions, are interpolated to an equidistant grid in  $\rho$ .

The first parameter represents the significance of a crash event:  $A_{norm} = A_{crash}/A_{rad}$  with

$A_{crash} = \int_{-\rho_m}^{\rho_m} |p(\rho)| d\rho$  and  $A_{rad} = \int_{-\rho_m}^{\rho_m} s(t_{SC}, \rho) d\rho$  ( $s$ : original signal).  $A_{norm}$  might also serve as SC amplitude, however, it depends on the precrash profile shape, and a proper quantification is still to be studied. We found values as low as 2 % for inverted crashes in SXR. The second parameter is determined by the redistribution:  $A_{net} = |\int_{-\rho_m}^{\rho_m} p(\rho) d\rho| / A_{crash}$ . Redistribution means  $A_{net} < 1$ . For the case in figure 1, this criterion is sufficient to reject all FPs but accept all mode-preceded crashes. Another type of FPs arises from slow (1,1) mode oscillations with large growth rate. Since the (1,1) mode has opposite phase on different sides of the magnetic axis, crash profiles are strongly asymmetric for mode induced detections. The third parameter, therefore quantifies the profile asymmetry:  $p_{asym} = \sqrt{\int_0^{\rho_m} (p(\rho) - p(-\rho))^2 d\rho} / A_{crash}$ . Mode detections are rejected by the requirement  $p_{asym} \leq 1$ . A drawback is that also SCs that are preceded by a slow (1,1) mode can be rejected, depending on the mode phase at  $t_{SC}$ .

**Results and Outlook** Figure 3 shows an example of the SC detection with inverted crashes and strong variations. In the 37 discharge seconds studied in detail so far, using only one of the SXR cameras, we achieved very good rejection of FPs (1091) and acceptance of SCs, including inverted (1195), with only few accepted FPs (34,

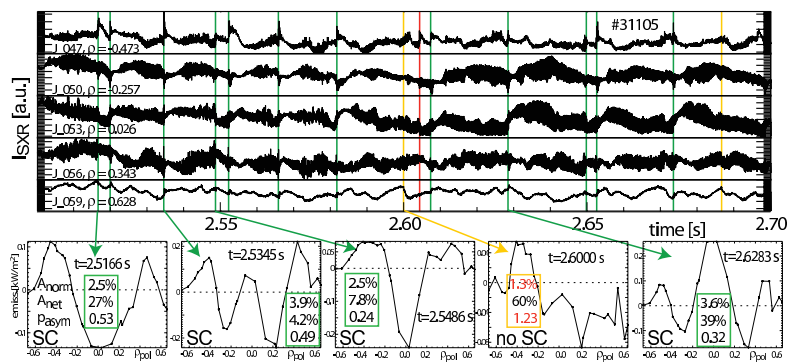


Figure 3: Some SXR time traces with detected SCs (green), rejected FPs (yellow) and 1 missed SC (red, too close to next SC); Below: some crash profiles with profile parameters.

most of which have  $A_{norm} < 3\%$  and are much smaller than the surrounding SCs) and rejected SCs (15). Crashes missed in the first step are not yet counted but scarce, and events that are difficult to decide (e.g., a fishbone that causes SC-like losses) are ignored. Note that despite a very broad range of heating and plasma parameters, we did not adjust any of our chosen parameters. These are: kernel length: 1.5 ms, kurtosis window: 12 ms, kurtosis threshold: 4.5, profile width:  $\rho_{pol} \leq 0.7$ , and for sawtooth crash acceptance:  $A_{norm} \geq 2\%$ ,  $A_{net} \leq 0.9$  and  $p_{asym} \leq 1$ . Rejected SCs so far were all preceded by a slow (1,1) mode, which in ASDEX Upgrade only occurs with low NBI heating power. Since the rejection depends on the mode phase, such crashes are accepted from SXR cameras with different viewing angles. Combining 2 or more cameras will therefore be a next step. Possible further steps are profile parameter refinement, replacing fixed acceptance thresholds by probability variation, preprocessing of signals, and an extended statistical investigation of detection reliability, including missed detections. Real-time implementation and application on tomographic reconstructions are foreseen for the future.

[1] A. GUDE et al., *Proc. 37th EPS Conf. Plasma Physics, Europhys. Conf. Abstr.*, **34A** P4.124, 2010

[2] M. SERTOLI et al., *Plasma Physics and Controlled Fusion* **57** 07500 (2015)

[3] J. CANNY, *IEEE Trans. on Pattern Analysis and Machine Intelligence*, **PAMI-8**, NO. 6, Nov. 1986

This work has been carried out within the framework of the EUROfusion Consortium and has received funding from the Euratom research and training programme 2014-2018 under grant agreement No 633053. The views and opinions expressed herein do not necessarily reflect those of the European Commission.